Sensors & Actuators: B. Chemical 393 (2023) 134313

Contents lists available at ScienceDirect

Sensors and Actuators: B. Chemical

journal homepage: www.elsevier.com/locate/snb

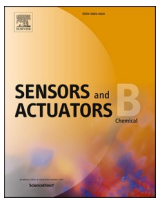

Selective detection of liposoluble vitamins using an organic electrochemical transistor

Luca Salvigni [a,b], Federica Mariani [b,*], Isacco Gualandi [b], Francesco Decataldo [c], Marta Tessarolo [c], Domenica Tonelli [b], Beatrice Fraboni [c], Erika Scavetta [b]

[a] Organic Bioelectronics Laboratory, Biological and Environmental Science and Engineering Division (BESE), King Abdullah University of Science and Technology (KAUST), Thuwal 23955-6900, Saudi Arabia
[b] Dipartimento di Chimica Industriale 'Toso Montanari', Università di Bologna, Viale Risorgimento 4, 40136 Bologna, Italy
[c] Dipartimento di Fisica e Astronomia, Università di Bologna, Viale Berti Pichat 6/2, 40127 Bologna, Italy

ARTICLE INFO

Keywords:
Lipophilic vitamin
Retinyl acetate
Tocopherol
Organic electrochemical transistor
Electrochemical sensor
Vitamin detection

ABSTRACT

Accurate quantification of vitamins content is essential in food analysis, with direct impact on the quality of our diet and, therefore, on our health. Current research interest is devoted to the design of robust and versatile devices able to perform real-time analyses that do not strictly rely on laboratory facilities. Here, we report the first organic electrochemical transistor (OECT) based sensor working in organic environment for the detection of a fat-soluble vitamin (Vitamin A). The OECT behaviour in organic solvents was thoroughly characterized and its structure was optimised allowing both potentiostatic and potentiodynamic detections. On one hand, the potentiostatic approach provided a gain of 100 and the detection limit was as low as 115 nM, but it did not address selectivity issues. On the other hand, the potentiodynamic approach showed a higher detection limit, but allowed the selective detection of Vitamin A in the presence of α-Tocopherol. Analyses of randomized solutions revealed that a pre-calibrated sensor can estimate Vitamin A concentration with a 3% error. Moreover, the robustness of our sensor was demonstrated by analysing commercial food fortifiers without any sample pre-treatment.

1. Introduction

Vitamins are essential to maintain a healthy metabolism and, among the most consolidated analytical methods for their quantification, the electrochemical route is the most advantageous approach for their real-time detection in food products. However, due to the complexity of the matrices, food analysis is mostly limited to the laboratory environment under controlled experimental conditions, thus making the development of multisensing platforms and portable devices a currently relevant research topic.

Vitamins are a specific class of organic compounds that are essential for the correct functioning of our body, but need to be supplemented via food or pharmaceutical sources, either because they are not endogenously synthesised at all, or due to the fact that their production inside the body does not cover the required intake [1]. Accurate quantification of vitamins content in commercial products is of great importance due to the heath-related problems that might originate from unbalanced diets, where excess or deficiency of vitamins occur [2]. As it is well known, almost all vitamins are electrochemically active and some of them exhibit antioxidant ability [3]. According to their solubility properties, they are usually divided into water-soluble, such as vitamins B and C, and fat-soluble compounds, including vitamins A, D, E and K [4]. While most of the official procedures, e.g., microbiological assays, are outdated, time consuming and relatively unprecise, the most routinely employed analytical technique is liquid chromatography, even if spectrophotometric, fluorimetric and electrophoretic methods have been reported [2,5]. Thanks to their lower cost, lower amount of sample required, ease of miniaturization and higher speed of analysis, electrochemical techniques stand as an advantageous alternative and there is, in fact, great research activity in the design of novel electrochemical transducers and sensing strategies [4].

A SiO_2/graphene oxide/$Ni(OH)_2$ modified glassy carbon electrode [6] and a Nitrogen-doped carbon nanotubes based sensor [7] were developed for the detection of Vitamin D3 in buffered solutions showing nanomolar and picomolar detection limits using differential pulse voltammetry and cyclic voltammetry, respectively. Folic acid detection in

* Corresponding author.
E-mail address: federica.mariani8@unibo.it (F. Mariani).

https://doi.org/10.1016/j.snb.2023.134313
Received 27 March 2023; Received in revised form 3 July 2023; Accepted 17 July 2023
Available online 20 July 2023

fortified milk samples has been recently reported using an indirect competitive immunoassay, exploiting a secondary-enzyme labeled antibody to transduce the chemical signal at a magnetosensor [8]. Comparable detection limits were found with a magneto-ELISA method using an optical transduction. A Hydroxyapatite-ZnO-Pd NPs modified carbon paste electrode was designed for the simultaneous detection of arbutin and vitamin C using differential pulse voltammetry [9]. With a response time shorter than 5 min, the sensor capabilities were demonstrated analyzing fruit juice and lightening cream samples. In the last 3 years, few proof-of-concept studies concerning the design of portable sensing platforms have been reported as well. A self-powered textile sensor based on polyaniline/reduced graphene oxide [10] has been developed for the detection of vitamin C beverages, showing promising application values in daily nutrition track necessities. An electrochemical aptasensor modified with graphene quantum dots/Au hybrid nanoparticles was employed for vitamin D3 quantification, with sub-nanomolar detection limit via impedimetric detection, which was integrated with controlled electronics to build a portable prototype [11]. Finally, J. R. Sempionatto et al. have recently reported on a pioneering work concerning a wearable biosensing platform integrated into an eyeglasses nose-bridge pad for multianalyte detection in tears, including alcohol, glucose and vitamins B2, C and B6 [12]. In that work, screen-printed carbon electrodes were used for vitamins detection through square wave voltammetry (SWV), thus demonstrating the first non-invasive monitoring of vitamins towards potential personal nutrition applications. Concerning the simultaneous analysis of multiple vitamins, the determination of the total antioxidant capacity has been largely investigated using electrochemical sensors [13,14] and the individual antioxidant activity of hydrophilic and lipophilic vitamins has been simultaneously measured using bicontinuous microemulsions [15].

Alternative to the conventional electrochemical sensing architectures, organic electrochemical transistor (OECT) based sensors have been gaining momentum in the bioelectronic scenario in the last decades [16–19]. OECTs are electrolyte-gated transistors where the channel material is an ion-permeable organic semiconductor, usually poly(3, 4-ethylenedioxythiophene):polystyrene sulfonate (PEDOT:PSS), connecting source and drain electrodes. The gate electrode, which can be either metal or polymer based, is in contact with an electrolyte solution and its potential (V_g) drives ionic fluxes across the solution and throughout the bulk of the polymer channel, whose redox state is reversibly varied through electrochemical doping. These phenomena lead to the extraction/injection of the charge carriers (holes, $PEDOT^+$) that allow an electronic current (I_d) to flow across the channel upon application of a potential to the drain electrode (V_d) [20]. The potential of OECTs to create powerful bioelectrochemical interfaces has been proven so far with the development of neuromorphic devices [21,22], cells monitoring platforms [23–26] and chemical sensors [27–29]. In particular, as long as (electro)chemical reactions involving a target chemical species interfere in the redox phenomena ruling the OECT, it can be used as an electrochemical sensor and I_d can be exploited for detection. Moreover, thanks to the interplay of transducing and amplifying units in the transistor architecture, OECT based amperometric and potentiometric sensors have been reported, which have been shown to outperform the analytical response of the simple electrochemical transducer [28–31]. On one hand, well-assessed functionalization strategies and electrochemical techniques have been adapted and exploited to develop OECT sensors for biologically relevant molecules with boosted analytical performance. On the other hand, the versatile transistor structure, its compatibility with common microfabrication techniques, the low power consumption and the absence of a reference electrode have significantly expanded the number of applications accessible to electrochemical sensors, including wearable electronics [32,33]. However, vitamins detection remains a rather unexplored field, where OECT based sensors have been reported for Vitamin C sensing only [34–37]. Thanks to the electrocatalytic properties of PEDOT, oxidative detection of Vitamin C has been demonstrated with all-PEDOT:PSS OECTs either exploiting potentiostatic [34] and potentiodynamic [35] approaches, the former allowing to reach a detection limit of 10^{-8} M in buffer solution and the latter guaranteeing selective detection in the presence of other oxidizable molecules. Another label-free, screen-printed OECT sensor has recently been reported for the analysis of Vitamin C in commercial fruit juices, showing a good agreement with the Vitamin content determined by HPLC and with the values reported in the literature [36]. Finally, an OECT sensor equipped with a molecularly imprinted polymer-modified gate electrode for the analysis of Vitamin C-rich beverages was reported, reaching a 10 nM detection limit [37]. In conclusion, ascorbic acid is the only vitamin detected with OECT sensors so far. Moreover, there is no paper in the literature reporting the application of OECTs in the analysis of non-aqueous environments and the sensing of fat-soluble analytes, whereas the transistor behavior in aqueous solutions has been well-documented [38–40].

In this work, we describe the development of an OECT-based electrochemical sensor for the selective detection of Vitamin A in the form of retinyl acetate (RETA). Being a fat-soluble vitamin, the need to use organic electrolytic solutions has required us to first carry out a thorough characterization of both the electrode material and the device behavior. The device structure and the analytical technique have been optimized in order to achieve the selective detection of retinyl acetate in the presence of α-Tocopherol (Vitamin E) in the organic solvent. Eventually, the robustness of our sensor has been demonstrated with the analysis of commercial food fortifiers, in which Vitamin A content was successfully determined with no sample treatment needed.

2. Materials and methods

2.1. Materials and chemicals

CLEVIOS™ PH 1000 suspension (PEDOT:PSS) was purchased from Heraeus. Ethylene glycol (EG), 3-glycidoxypropyltrimethoxysilane (GOPS), 4-dodecylbenzenesulfonicacid (DBSA), ethanol (96%), acetonitrile, lithium perchlorate, retinyl acetate (RETA), retinyl palmitate (REPA) and α-tocopherol (TCF) were purchased from Sigma Aldrich. Silicone elastomer and curing agent for the preparation of PDMS were obtained from Sylgard. RETA 325 CWS/A, REPA 250 S/N, Dry Vitamin E CWS/S, Ascorbic Acid FP 0422460 and the multivitamin premix were provided by DSM Nutritional Products.

The organic solvent employed during all the tests was a 1:1 v/v mixture of ethanol (96%) and acetonitrile with 0.1 M lithium perchlorate.

2.2. Fabrication and morphological characterization of the OECT sensor

Glass substrates were cleaned by sonication in distilled water/acetone/isopropanol baths. Afterwards, 10/30 nm of Cr/Au were deposited by thermal evaporation, realizing the contact pads and conductive tracks of the device. PEDOT:PSS solution was then spin coated to realize the device channel and gate electrodes, using a Teflon mask: 500 rpm for 30 s and 3000 rpm for 10 s were set as spin coating recipe for the thick (600 ± 90 nm) and thin (170 ± 10 nm) film realization. The solution was made of 93.75% PEDOT:PSS (Heraeus, Clevios PH1000) with 5% EG, 1% GOPS and 0.25% DBSA. This suspension was treated in ultrasonic bath for 10 min and filtered through 1.2 μm cellulose acetate filters (Sartorius) before the deposition. The samples were subsequently baked at 120 °C for 1 h. The resulting OECTs dimensions were: channel length (L) and width (W) of 11 and 3 mm, respectively, with the gate electrode having L = 4 mm and W = 3 mm. Finally, the devices were merged in distilled H_2O for 1 h, dried with nitrogen flux and Polydimethylsiloxane (PDMS) was deposited on the interconnects, correctly patterning the active areas of the devices. The morphology characterisation was carried out in air at room temperature in tapping

mode with an atomic force microscopy (AFM) Park System NX10 (Park System, Suwon, Korea).

2.3. Electrochemical and electrical characterization

Cyclic voltammetry (CV) experiments were carried out in a three-electrodes cell endowed with a Pt wire counter electrode, a saturated calomel electrode (SCE) as a reference electrode and, as a working electrode, either (i) PEDOT:PSS or (ii) Au thin films deposited on a glass slide. The electrochemical responses were acquired employing a CH Instruments 660 C potentiostat.

The OECT electrical characterizations (output and transfer curves) were carried out using a Keysight B2902A source meter unit, by applying drain (V_d) and gate (V_g) voltages and measuring the drain (I_d) and gate (I_g) currents.

The electrochemical potentials of the OECT elements were measured with the setup reported in the Supporting Information (Fig. S5a), by simultaneously employing the source meter to apply V_d and V_g and the potentiostat to measure the source electrochemical potential (E_s). The drain and gate electrochemical potentials were calculated by adding V_d and V_g to E_s, respectively. For the static measurements (Fig. 2a), three minutes V_g pulses were applied while a constant V_d was kept in order to reach a stable E_s. For the dynamic measurements (Fig. 4c and others) instead, the V_g was linearly scanned at the desired scan rate.

2.4. Vitamins sensing

For vitamins sensing the OECT was immersed in the organic solvent and the electrochemical measurements were carried out as follows. For the potentiostatic measurement, the solution was kept under magnetic stirring, and constant V_d and V_g were applied while I_d and I_g were recorded. After the I_d stabilization, controlled vitamins amounts were gradually added to the electrolyte.

For the potentiodynamic measurement, the transfer curves were acquired in quiescence after addition and mixing of different vitamins amounts. The OECT performance was evaluated in terms of sensitivity, limit of detection (LoD), response time, accuracy and signal to noise ratio (S/N).

The LoD values were calculated using the 3σ/m criterion (where σ is the standard deviation of the blank and m is the slope of the calibration curve), according to [41].

3. Results and discussion

3.1. Material characterization in the organic solvent

The first step in the development of a sensor for liposoluble vitamins operating in organic environment was the electrochemical characterisation of the electrode materials in a solution of EtOH:CH_3CN 1:1 containing 0.1 M $LiClO_4$ as the supporting electrolyte. While methanol is one of the most common liquid chromatography solvents in the analysis of vitamins [42], we chose the less harmful ethanol in a mixture with acetonitrile, which is a standard solvent in electrochemistry. The materials under investigation were spin-coated PEDOT:PSS films and evaporated Au films, as described in the Experimental section, which were selected since they are commonly used for the fabrication of OECTs operating in aqueous environment. First, the stability and electrochemical behaviour of PEDOT:PSS in the organic environment were studied by CV (Fig. 1a). A rather wide electrochemical potential (E) window was identified, where the polymer is electrochemically stable and shows a purely capacitive behaviour, ranging from − 0.31 to 0.85 V vs SCE. Working within this range avoids side reactions to occur [34], as well as overoxidation promoted by the organic solvent to take place.

Fig. S1 shows the CV measurements recorded at PEDOT:PSS and Au

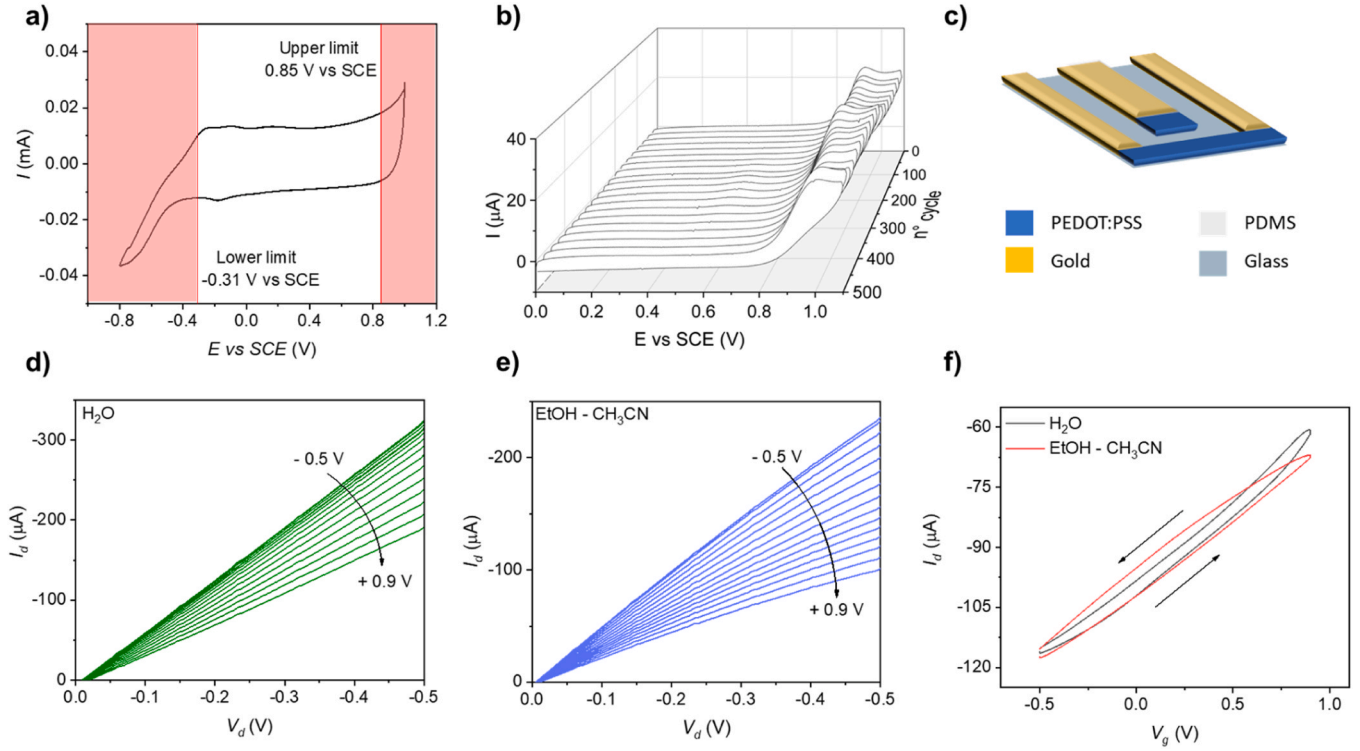

Fig. 1. Material and OECT characterization in the organic environment. (a) CV of a PEDOT:PSS thin film in organic solvent in an extended potential range and identification of the stability window, delimited by the red bars, scan rate: 50 mV/s; (b) 500 cycles of CV of a PEDOT:PSS working electrode at 100 mV/s in organic solvent containing 1 mM RETA; (c) Final device structure after materials optimization; (d) OECT output curves in aqueous solution containing 0.1 M $LiClO_4$ at 30 mV/s, with V_g ranging from − 0.5 to + 0.9 V (step 100 mV); (e) OECT output curves in organic solvent at 30 mV/s with V_g ranging from − 0.5 to + 0.9 V (step 100 mV); (f) OECT transfer curves in aqueous solution and organic solvent, both containing 0.1 M $LiClO_4$ as the supporting electrolyte, at 30 mV/s. V_d = −0.2 V.

working electrodes in the organic solution containing 1 mM RETA. Retinol and its ester derivatives undergo a similar oxidation process [43], which has been described as chemically irreversible as only a forward oxidative peak is typically observed during CV measurements; however, retinoids have been reported to undergo reduction processes on Pt or on Hg/Pb coated electrodes at about − 2 V vs SCE in organic solvent [44]. The mechanism of the electrochemical oxidation has not been clarified yet, but up to five steps have been identified during DPV measurements [45]. Based on electrochemical, quantum-chemical calculations and FTIR analysis, it has been proposed that the electrooxidation of retinyl esters involves the exchange of two electrons and one H^+ [46] and the oxidation should be delocalized over the 5 carbon atoms of the π-conjugated system [45]. The irreversible oxidation of RETA starts at about 0.70 V vs SCE at the PEDOT:PSS electrode, i.e. within the stability window of the polymer. In the case of the Au electrode, a higher current density was recorded with an anticipation of the oxidation potential equal to 0.07 V. The long-term stability and fouling phenomena were investigated by monitoring the shape, position and intensity of the RETA oxidation peak during 500 cycles of CV. The response obtained for the Au electrode is reported in Fig. S2a and shows that the RETA oxidation peak disappeared after 215 cycles. Instead, a constant and very stable response is recorded for the PEDOT:PSS electrode during the whole analysis (Fig. 1b). As presented in Fig. S2b, the intensity of the oxidation peak remains fairly constant and stable for both materials within the first 215 cycles, however, only PEDOT:PSS shows remarkable consistency even in the peak position, as evident from Fig. S2c. In fact, gold suffers from a continuous and progressive anodic shift of the oxidation peak. Overall, the electrochemical instability of the Au film in organic environment is likely due to the delamination of the metal from the support following morphological changes upon cycling [47], as confirmed from the comparison of the AFM images of Au (Figs. S2d-f) and PEDOT:PSS (Figs. S2g-i) electrodes.

3.2. Design and characterization of the OECT in the organic environment

Material characterization highlighted that PEDOT:PSS exhibits superior stability in the presence of the redox active analyte and does not suffer from any fouling effect, if compared to evaporated Au films. For these reasons, we chose PEDOT:PSS to fabricate both the main transistor elements, e.g., the gate and channel. A schematic of the resulting device is presented in Fig. 1c. The planar geometry of choice comprises an inner gate electrode and an U-shaped channel, both of them deposited during a single-run spin-coating step of the organic semiconductor, which was patterned to achieve the desired gate to channel area ratio (γ). On one hand, this OECT architecture facilitates the immersion of the device in the electrolytic solution during the analyses [34,48]. On the other hand, since the role of γ in all-PEDOT:PSS OECTs working in aqueous environment had already been investigated by our group with respect to gating efficiency, amplification, as well as sensing capabilities [30,49], $\gamma = 0.3$ was originally chosen to investigate the OECT behaviour in the organic solvent.

With this device structure, we analysed the output and transfer characteristics and compared the response obtained in the organic solvent with that recorded in aqueous solution. The output curves acquired in aqueous and organic solvents are reported in Fig. 1d and e, respectively, and highlight that the device shows the expected transistor behaviour even in the organic solvent, allowing a wide drain current modulation upon gating across the electrolytic solution. Similarly to other millimetre sized channels in all-PEDOT OECTs [49], the linear regime is the dominant feature in the output curves.

Interestingly, the normalised output curves reported in Fig. S3 demonstrate that the organic solvent allows a higher gating than water. The effect is particularly evident at negative gate voltages, where the onset of the oxygen reduction reaction in aqueous environment likely anchors the electrochemical potential of the gate electrode. The comparison of the transfer curves (Fig. 1f) highlights another difference between the transistor behaviour in the two solvents, i.e., a slightly higher hysteresis obtained in the organic environment, which is probably due to the mass transport related to the ionic current that is slowed down by the lower conductivity of the organic solution.

Overall, these tests showed that the all-PEDOT OECT is compatible with the organic environment and can efficiently work as a transistor in experimental conditions of choice.

3.3. RETA detection

According to a recent report released by the European Food Safety Authority (EFSA) Panel on Dietetic Products, Nutrition, and Allergies [50], Vitamin A deficiency is rare in the Western world and a major problem in developing countries, however health consequences related to both its deficiency and excess are largely documented [51]. Considering dietary reference values (in μg retinol equivalent (RE) per day), the average requirement is 570 and 490 for men and women, respectively, while the tolerable upper intake level for preformed Vitamin A is set to 3000 for adults [50]. Retinyl acetate (RETA) and palmitate (REPA) are common retinoids employed for food fortification.

Once the capability of the all-PEDOT:PSS OECT to operate in the organic environment was assessed, we investigated its electrochemical behaviour and sensing performance for RETA determination. A potentiostatic technique was chosen to carry out the real-time detection of the analyte, in which fixed V_d and V_g are applied, while I_d is monitored over time during progressive RETA additions into the organic solution. This approach is simple, widely used in OECT sensing and, in analogy with chronoamperometric methods, it allows to reach high sensitivities and low LoDs [19,29,34]. Furthermore, it provides an easy control of the applied potentials, which must be optimised in order to reach the desired electrochemical potentials at the transistor interfaces and trigger the electrochemical event that will be transduced and amplified by the OECT sensor (RETA oxidation).

For the optimisation of V_d and V_g, we initially measured the electrochemical potentials assumed by source, drain and gate at different applied V_d and V_g. The results are reported in Fig. 2a and the instrumental setup is illustrated in Fig. S4a. This measurement allows correlating the E value of the OECT interfaces (i.e., gate and channel) with the applied voltages. Based on the CV experiments shown in Fig. 1b, the aim of this investigation was the identification of the voltages needed to achieve a sufficiently oxidative E at the PEDOT:PSS gate or channel for RETA oxidation, starting at about 0.7 V vs SCE, without causing PEDOT:PSS overoxidation.

Based on the graph reported in Fig. 2a, RETA detection might be investigated in two conditions: (i) an oxidising channel, where the sensing and amplification processes occur on the same component and the gate electrode is used only to control the E value of the channel; (ii) an oxidising gate, which works as a sensing component, while the channel works as the signal amplifier [30,34,49].

When using the former condition (i), we rose the channel E using a negative gate voltage ($V_g < 0$), however the device did not show any significant current modulation upon RETA additions to the organic solvent (data not shown). This was probably due to the electrochemical potential gradient existing across the channel, between the source and drain electrodes [49], where the oxidative portion of the channel was not sufficiently extended for the transduction event to occur and, therefore, to produce a measurable signal. To further increase the channel E, either a more negative V_g or a more positive V_d should be applied. However, this setting would lead the PEDOT:PSS potential to fall outside its stability window. For these reasons, no further experiments were performed using this approach.

On the other hand, the detection of RETA at the gate electrode (ii) has proved to be successful. As reported in Fig. 2b, we performed the detection using two different thicknesses for the PEDOT:PSS film spin-coated at both gate and channel, e.g., 600 and 170 nm. All devices showed an evident current modulation after subsequent additions of

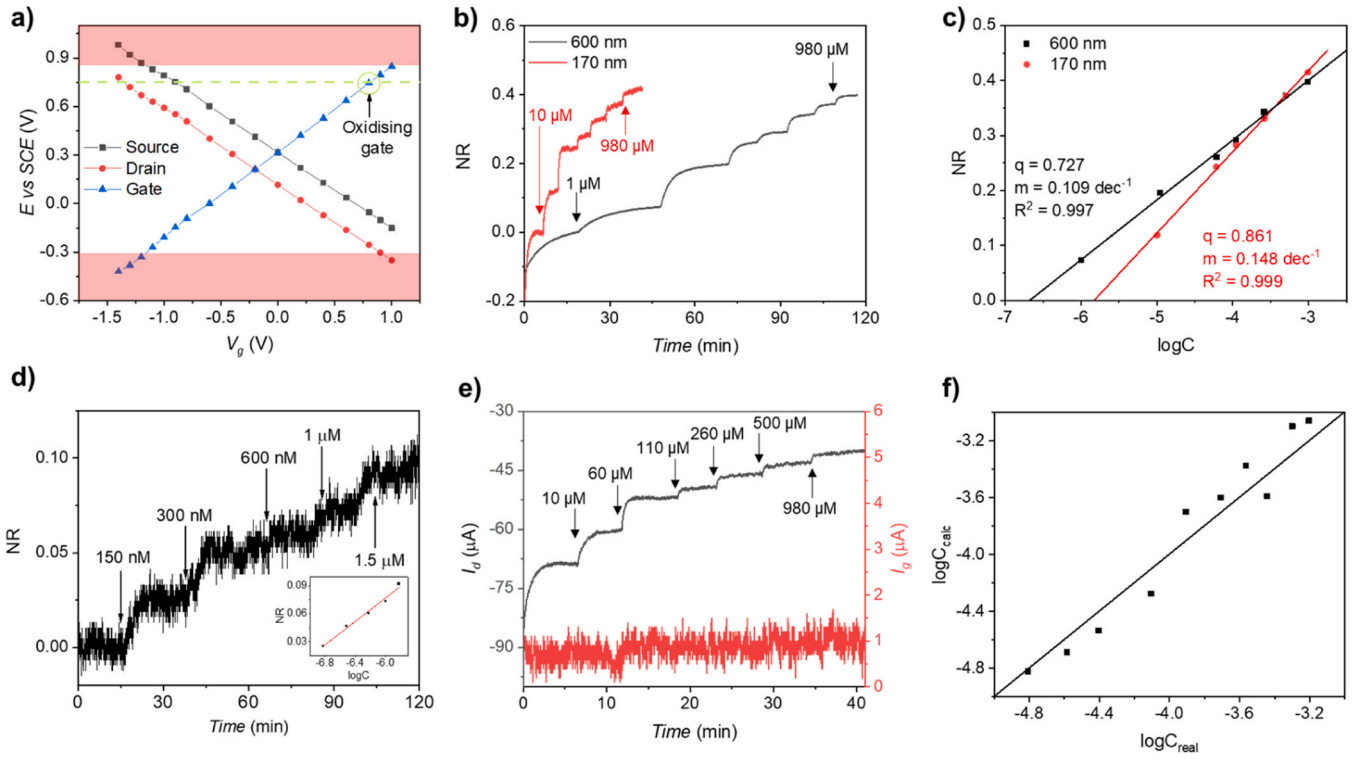

Fig. 2. Design of the all-PEDOT OECT sensor for RETA detection. (a) Electrochemical potentials of gate and channel at different applied gate voltages (potentiostatic) in the organic solvent, $V_d = -0.2$ V; the red bars delimitate the PEDOT:PSS stability window and the dotted green line represents the E value at which RETA oxidation starts, based on CV measurements; (b) Potentiostatic detection of RETA using the optimized voltage conditions ($V_d = -0.2$ V, $V_g = +0.9$ V) for OECTs with different PEDOT:PSS film thickness (NR = normalised current response); (c) Calibration curves of the potentiostatic measurements shown in panel b; (d) Potentiostatic detection of RETA (170 nm thick PEDOT) with concentrations close to the LoD value. Inset: calibration plot (calibration curve parameters: q = 0.45; m = 0.063; $R^2 = 0.980$); (e) Comparison of drain and gate currents during potentiostatic detection of RETA; (f) Simulation of a real sensor use by testing random RETA concentrations in the organic solvent and comparison between the calculated concentration with the real one.

RETA to the organic solution. The sensors responded with a logarithmic behaviour within the whole concentration range under investigation (1 µM ÷ 1 mM), showing very good linear correlation (calibration curves in Fig. 2c). However, at concentrations < 100 µM, the average response time (t_{90}) using the thicker polymer film was 15 min, then decreasing to 5 min at higher RETA concentrations. While 600 nm is a quite common thickness value when fabricating organic transistors, such response times are higher than those typically found for OECTs working in aqueous environment (e.g., around 1 min [34]). As anticipated when comparing the transfer curves, the long response time might be due to the lower conductivity of the organic solvent with respect to water, which consequently slows down the diffusion of ions across the ionic circuit of the OECT. The overall result is an increase in the time required by the polymer to reach an equilibrium condition and generate a flow of steady state current. However, the fact that the variation of charge carrier concentration in the conductive polymer involves the entire polymer bulk [52] explains the shorter response time obtained using the second OECTs, where the thinner PEDOT:PSS films (170 nm) significantly reduces the mean path of the diffusing ions. In fact, in this case the response time decreased to about 120 s for all the investigated RETA concentrations without any significant loss of sensing performance, as demonstrated by the sensitivities comparison (Fig. 2c).

Fig. 2d shows the response of the optimised device at the lowest concentrations, for which a LoD of 115 nM is obtained. From these results, we can assert that the device can efficiently work across four orders of magnitude of concentrations.

An important advantage provided by the OECT sensor is shown in Fig. 2e, where we compared the gate and drain currents. The gate current represents the direct oxidation current of the vitamin; therefore, it can be considered similar to the response of a conventional PEDOT:PSS-based amperometric sensor. The drain current, instead, represents the amplified signal due to the transistor configuration. Considering the 60 µM RETA addition, which was the only one clearly visible in both I_g and I_d vs time curves, we can observe the two main results obtained in the organic solvent: (i) the amplification provided by the OECT, also called gain ($\Delta I_d/\Delta I_g$) is close to 100, which means that the variation of the direct oxidation current (I_g) is amplified by two orders of magnitude by the transistor configuration; (ii) the signal to noise ratio (S/N, calculated using the steady state current variation recorded at 60 µM RETA and the standard deviation of the blank signal) increases from 1 for the direct signal, to 74 for the amplified signal. The latter result demonstrates how the Faradaic I_g signal, which is barely distinguishable from the background noise, becomes an useful analytical signal thanks to the amplification provided by the OECT, thus leading to a significantly larger working range towards lower concentrations.

To further support these assertions, we also compared the responses of the OECT sensor with that of a PEDOT:PSS working electrode, operating in a three electrodes cell (Fig. S5). In this case, the direct oxidation signal exhibits a S/N at 500 µM RETA that exceeds 1200 and is considerably less noisy than I_g, where the calculated S/N at the same analyte concentration was 1. However, while the classical electrochemical approach guarantees a 1.4 µM LoD, the OECT displays a LoD of one order of magnitude lower (115 nM). The obtained results clearly show the efficiency of the developed device for this new application, even if compared to a conventional and well-established electroanalytical technique.

As a last characterization test, the sensor accuracy was evaluated by comparing the logarithm of RETA concentration, calculated from the calibration curve, with the real value of synthetically prepared solutions (Fig. 2f). In order to introduce a stress factor and assess the reversibility

of the sensor response, we evaluated the accuracy by analysing different solutions with concentrations ranging over almost two orders of magnitude in a random order. The device showed an average error of 3.8%, indicating no significant memory effect and a remarkable accuracy, in agreement with the PEDOT:PSS long term stability and anti-fouling properties.

3.4. RETA detection in the presence of α-tocopherol as interfering species

As almost all fat-soluble vitamins that are present in food matrices are redox-active [4], selectivity is a common issue that electrochemical sensors should address.

Due to the vicinity of their oxidation potentials, the simultaneous detection of vitamins A and E [53], as well as of various fat-soluble vitamins (A, D, E and K) [54,55] have been achieved so far thanks to the combination of Carbon-based nanomaterials modified electrodes and one of the most sophisticated electroanalytical techniques, e.g., square wave voltammetry. In spite of the above discussed major advantages offered by the PEDOT:PSS OECT sensor, the transduction mechanism based on RETA oxidation at the polymeric gate electrode may not be effective in discriminating among other oxidizable molecules. For this reason, we thoroughly investigated the selectivity of the developed sensor for RETA detection by introducing α-tocopherol (TCF) into the organic environment.

The comparison of CVs recorded in the organic environment containing only RETA and a mixture of RETA and TCF in equal concentrations is presented in Fig. 3a. TCF oxidation takes place at lower E than RETA ($\Delta E = -0.2$ V), thus suggesting that the potentiostatic technique could not be selective. In fact, in a mixture of the two vitamins, the current recorded at the potential required for RETA oxidation would also comprise the TCF oxidation signal, with TCF acting as interfering agent.

The potentiostatic OECT response in the presence of TCF using the experimental conditions optimised for RETA detection and a comparison of the sensor performances during RETA and TCF calibrations are presented in Fig. S6 and Fig. 3b, respectively. It clearly stands out that TCF interferes not only due to its lower oxidation potential, but also inducing a stronger OECT current modulation, thus making TCF a model interfering component for our investigation. While in the low μM range (up to 4 μM TCF) the sensor response is linear, the logarithmic response obtained for TCF concentrations up to 100 μM gives a 3.5 times higher sensitivity if compared to RETA. Above 100 μM TCF, the sensitivity becomes very similar to RETA, but the drain current response is 2.3 times higher.

The effect of the analyte-OECT interplay can be seen from an electronic point of view as a variation of effective V_g that acts on the channel, which is called V_g offset [56]. Fig. 3c shows the V_g offset recorded in the organic solution containing RETA or TCF at different concentration (V_g offset was extracted calculating the necessary voltage shift needed to overlap OECT normalized response at different analyte concentrations with the blank curve; more details are given in Fig. S7). TCF gating effect is 3.3 times higher than RETA gating contribution. Overall, these preliminary tests highlight that TCF behaves as a strongly interfering molecule due to (i) the lower oxidation potential and (ii) the higher gating capacity, thus representing a relevant benchmark species for selectivity studies.

Considering the state-of-the-art PEDOT:PSS based OECT sensors, the most common approach to impart the desired selectivity is to functionalise the electrochemical interface where the transduction takes place. However, this approach implicates additional fabrication steps and raises the complexity of the sensing platform, which is not desired in view of the design of low-cost, low-maintenance devices. An alternative strategy that allows to either suppress or separate the contribution of the interfering species from the analytical signal is the design of a suitable potential profile or waveform to bias the OECT.

Following this approach, we first verified the possibility to subtract the TCF interference using a pulsed V_g profile (Fig. S8). In particular, V_g^{low} should only trigger the oxidation of TCF, while V_g^{high} should cause the oxidation of both components, allowing at first a quantification of the TCF alone and then its subsequent subtraction from the signal recorded at V_g^{high}. The OECT sensor was calibrated for RETA, TCF and RETA in the presence of 100 μM TCF (Fig. S9). However, by looking at the resulting calibrations of RETA and TCF, it clearly stands out that the two species give non-negligible contributions at both V_g^{high} and V_g^{low} and the use of the pulsed voltage profile fails in solving the selectivity issue. Therefore, the potentiostatic approach was definitively abandoned.

In a previous work [35], we optimised a potentiodynamic method to selectively detect dopamine with an all-PEDOT:PSS OECT sensor in an aqueous mixture containing uric acid and ascorbic acid. Taking into account the CV recorded in the mixture of the two vitamins where the two redox waves can be clearly identified (Fig. 3a), we applied an analogous voltage profile at the OECT gate electrode. Upon application of a potentiodynamic V_g in the presence of an oxidisable molecule, the gate current typically reflects the analyte oxidation profile, while the drain current undergoes the effect of this extra charge injection. The device transconductance ($g_m = \partial I_d / \partial I_g$) is an important figure of merit for OECTs and can be taken as the analytical signal: it reflects and amplifies the oxidation occurring at the gate electrode in the form of a peak, whose intensity can be quantitatively correlated with the analyte concentration. At first, the experimental conditions optimized in aqueous environment ($V_d = -0.3$ V, Scan rate = 2 mV/s [35]) were not effective for this new application as the OECT sensor was not able to discriminate the two vitamins, neither at the sensing electrode (gate), nor at the amplification system (channel), as shown in Fig. S10. Therefore, a

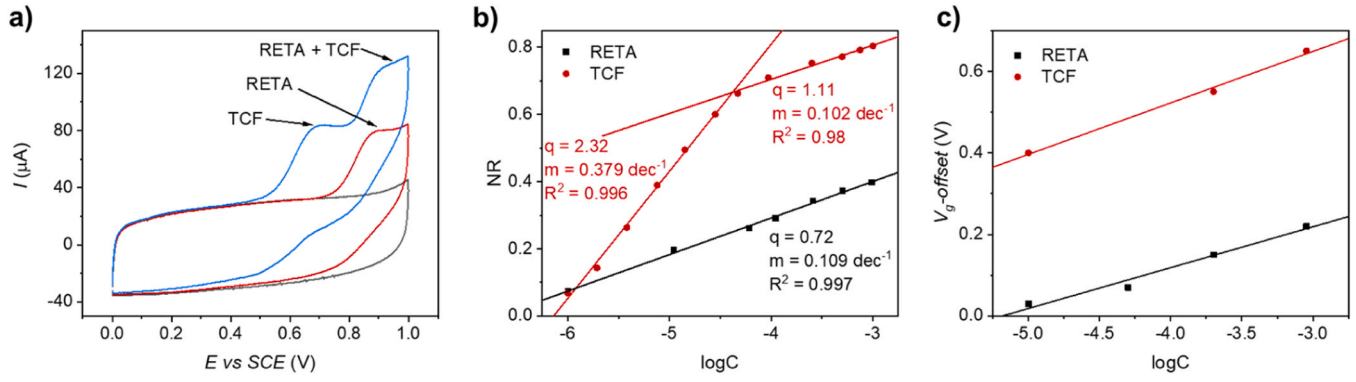

Fig. 3. Interference of α-tocopherol. (a) CV of 1 mM RETA (red curve) and a mixture of RETA and TCF, both 1 mM (blue curve) recorded in the organic environment using a PEDOT:PSS working electrode, scan rate 10 mV/s. Black curve: blank. (b) RETA and TCF calibration curves obtained with the OECT in potentiostatic mode as optimised for RETA detection ($V_d = -0.2$ V, $V_g = +0.9$ V); (c) Correlation of the offset V_g and analytes concentration.

kinetic study was carried out in order to better understand the device operation and the dynamics of the transduction processes at the OECT sensor when using the potentiodynamic mode. With this aim, both PEDOT:PSS and bulk Au were investigated as gate materials.

We initially analysed the vitamins oxidation in the organic environment by CV, recorded at different scan rates using a three electrodes cell setup. While RETA oxidation peak showed a regular behaviour with both PEDOT:PSS and gold electrodes (Fig. S11), TCF instead produced in both cases an irregular current profile for the lowest scan rates, exactly at the voltages at which RETA oxidation peak is expected (Fig. 4a and Fig. S12). This irregular shape is likely generated by the decomposition of TCF by an overall electrochemical process involving two consecutive redox reactions and/or chemical reactions promoted by the presence of H_2O traces in the organic environment and H^+, which may also favour the consecutive reaction of a third electron transfer to obtain the final oxidation product [57]. All these phenomena are kinetically slow and can be suppressed with a high scan rate. As shown in Fig. 4b, this strategy also helped to reduce the TCF interference at the RETA oxidation potential when a mixture of the vitamins is analysed. Thus, in order to reduce interfering signal of TCF, we chose a fast scan rate (100 mV/s) for the potentiodynamic technique applied to the OECT.

Then, the OECT behaviour at different scan rates was investigated. In particular, we measured the electrochemical potentials of the device elements in analogy with the measurements reported in Fig. 2a, but in a dynamic mode (i.e., linearly sweeping the gate potential). The aim was to verify that the application of a linear scan of V_g was effectively associated with a corresponding linear scan of the electrochemical potential of the OECT components, similarly to a CV. We found that the gate electrode efficiently follows the applied voltages at any scan rate, for both PEDOT:PSS (Fig. 4c) and the bulk Au (not reported) gate electrodes. The major difference between OECTs with a Au or PEDOT:PSS gate electrode is highlighted in Fig. 4d and regards the electrochemical potential of the channel. Thanks to the lower capacity of gold, the charges injected from the gate to the channel (leakage current, I_g) are significantly lower if compared to a PEDOT:PSS gate electrode. The result is that the E of the channel is just slightly affected by the gold gate electrode and the channel itself behaves not only as the transistor amplification system, but also as a good internal reference system for the gate, acting like a pseudo reference. The effect of this implication is reported in Fig. 4e and f. In particular, Fig. 4e shows the difference in the TCF oxidation potential between PEDOT:PSS and Au working electrodes in a three-electrodes cell. In this case, the peak shift is very small and can be ascribed to the different charge transfer properties of the two materials, where Au seems to facilitate TCF oxidation. On the other hand, analysing the gate current when the OECT configuration is used (Fig. 4f), i.e., in a condition where the Au and PEDOT:PSS working electrodes are used as gate electrodes and combined with a PEDOT:PSS channel, this potential shift is almost four times higher and the same holds at any scan rate (Fig. S13). The reason is that the applied gate voltage is referred to the grounded source electrode, whose potential in turn relates to the E of the channel, which progressively decreases as V_g increases when a PEDOT:PSS gate is used and a higher amount of charge is injected. Instead, with a gold gate electrode, E channel remains fairly constant (Fig. 4d). Consequently, at the same V_g, the electrochemical potential of the gate is lower for PEDOT:PSS, i.e., the sensing interface is less oxidative, thus causing an overall anodic shift of the current profiles. Therefore, a higher V_g must be applied to reach the same oxidative behaviour as gold, thus requiring a higher amount of energy and, at the same time, the channel is pushed beyond its lower limit of stability (−0.31 V vs SCE, see Figure1a), eventually reducing the device durability.

For all these reasons, the optimised sensing conditions of choice are the following: (i) an OECT with a thin channel of PEDOT:PSS (170 nm) to achieve a fast current modulation, (ii) a high scan rate (100 mV/s) to minimize the TCF interfering signal and interfering reactions and (iii) a gold gate electrode, which allows the device to work within its stability

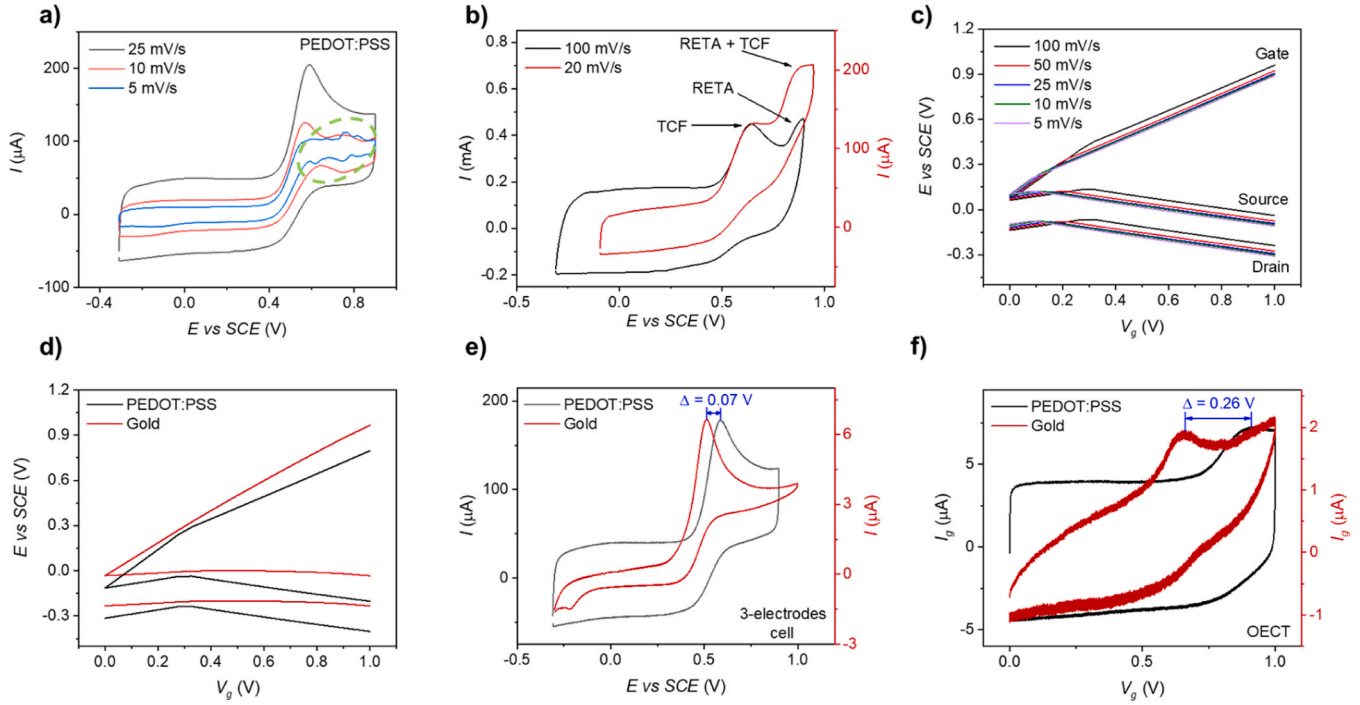

Fig. 4. Optimization of the OECT sensor in the potentiodynamic mode. (a) CV of a PEDOT:PSS electrode in 1 mM TCF at different scan rates, the dotted green circle highlights the irregular current shape; (b) CV of a PEDOT:PSS electrode in 1 mM RETA and a mixture of 1 mM RETA and 1 mM TCF at different scan rates; (c) from top to bottom, gate, source and drain electrochemical potentials during a potentiodynamic scan at different scan rates; (d) OECT electrochemical potentials obtained using PEDOT:PSS (black lines) and gold (red lines) gate electrodes during a potentiodynamic scan; (e) CV of 1 mM TCF in a three-electrodes cell using PEDOT:PSS and gold working electrode; (f) gate current of a potentiodynamic measurement with the OECT in the presence of 1 mM TCF using PEDOT:PSS or gold gate electrodes.

range, reduces the energy absorption and provides a sufficiently oxidising sensing interface. The optimised OECT configuration (Fig. 5a) successfully resolved the two vitamins redox waves, as reported in Fig. 5b. In the top panel of Fig. 5b, the gate current highlights clearly the presence of the two peaks, similarly to a CV, due to the oxidation of the two redox-active compounds. In the middle panel, we report the effect of this Faradaic process on the drain current, which is one order of magnitude higher than I_g. This represents an advantage as to the device construction, because it is easier and less expensive to build an electronic readout capable to measure hundreds of μA instead of few units of μA. Lastly, in the bottom panel of Fig. 5b, we report the transconductance vs V_g plot, which clearly resolves the signals ascribed to the two vitamins. With the Au gate electrode chosen for the potentiodynamic approach, the ratio between gate and channel areas of choice was 0.09, as it led to an OECT sensor working in a wide concentration range, which is analogous to that obtained with the potentiostatic technique (from μM to mM). A full RETA calibration and the sensor response to RETA in the presence of 100 μM TCF are reported in Fig. S14 and Fig. S15, respectively. Similarly to the potentiostatic technique, the device showed different response regimes, in particular a linear response for the lowest concentrations (Fig. S14b) and a logarithmic response for the highest concentrations (Fig. S14c).

The calculated LoD corresponds to 10 μM, which is two orders of magnitude higher than the value measured by the potentiostatic technique. Nevertheless, this result is widely compensated by the high selectivity achieved. In fact, we compared a RETA calibration in the presence and absence of 100 μM TCF (Fig. 5c). The corresponding calibration curves resulted identical according to statistical tests (t-test and F-test), thus demonstrating that the developed device entirely eliminated the TCF interference, without requiring any signal post-processing or sample pre-treatment. Overall, these results prove that a selective response can be obtained by the fine optimisation of both the transistor components and the potentiodynamic wave. The sensor discriminates electroactive vitamins thanks to the different thermodynamics and kinetics of their oxidation mechanisms, with no need of expensive electrode modifiers and avoiding more sophisticated waveforms than just a linear potential ramp.

Considering the gate current during the potentiodynamic analysis (Fig. S16), which is the direct oxidation current similar to the response expected in a CV, the presence of TCF causes a non-negligible interference on the detection of RETA. Furthermore, the RETA LoD (without TCF) is 100 μM, if I_g is used as the analytical signal. This result demonstrates that the OECT configuration guarantees not only an intrinsic signal amplification that leads to a LoD improvement of one order of magnitude (100 μM using I_g vs 10 μM using g_m), but also improves the signal resolution, eliminating the TCF interference from the RETA signal.

The accuracy of the potentiodynamic method was evaluated using random RETA additions (Fig. 5d). In the optimised conditions, RETA concentration can be estimated with an average error of 3%. Another important improvement provided by this method, if compared with the potentiostatic one, is that it is not necessary to normalize the signal with respect to the blank solution, but the calculated transconductance can be directly used to estimate RETA concentration. In this case, the analytical signal is in fact the I_d variation with respect to the applied potential (i.e., g_m), therefore, small changes in the PEDOT:PSS initial redox state do not significantly affect the transconductance variations related to the vitamins oxidation.

3.5. Stability, reproducibility and comparison with other electrochemical sensors

The stability of the OECT-based sensor was tested during repeated potentiodynamic cycles in the organic environment in the presence of 1 mM RETA (Fig. S17). The value of the analytical signal, g_m, at a V_g of 1 V remained stable at 43 ± 3 μS for up to 90 cycles at 100 mV/s. The multi-step fabrication process described in the Material and Methods section is a limiting factor for (i) scalability and (ii) reproducibility of the OECT sensors (Fig. S18a). In order to overcome this limitation, we used photolithography to scale down the transistor dimension maintaining the γ value (0.09) and the PEDOT:PSS thickness (170 nm) unaltered. The resulting microfabricated devices (L = 3800 μm, W = 900 μm) are obtained with a scalable, high-throughput approach and exhibit considerably improved reproducibility (Fig. S18b), thus allowing a calibration-free use of sensors belonging to the same batch.

The figures of merit of the OECT sensor are summarised in Table 1 and compared with other electrochemical sensors for the detection of Vitamin A. Very low detection limits have been obtained with

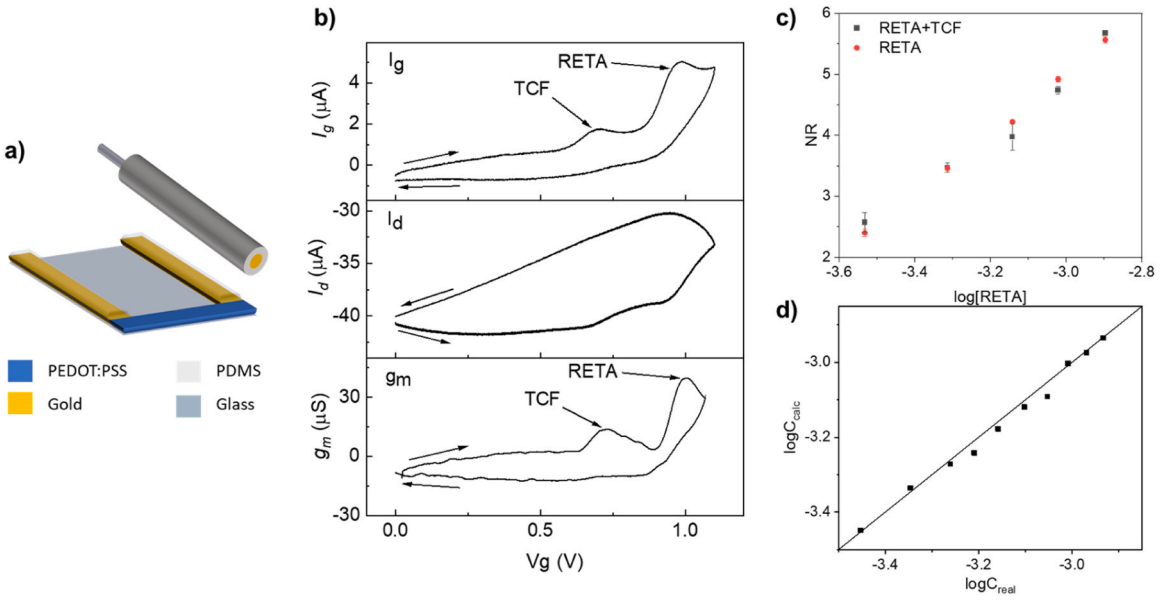

Fig. 5. Selective detection of RETA. (a) Layout of the OECT sensor equipped with the Au gate electrode. b) Potentiodynamic scan at $V_d = -0.2$ V and 100 mV/s for a mixture of 100 μM TCF and 500 μM RETA. On the top the gate current, in the middle the drain current and at the bottom the corresponding transconductance; (c) Potentiodynamic RETA calibration in presence and absence of 100 μM TCF (error bars represent the standard deviation calculated for N = 3 potentiodynamic cycles); (d) Simulation of a real sensor use by testing random concentrations of RETA and comparing the calculated concentration with the real one.

Table 1
Comparison among state-of-the-art electrochemical sensors for Vitamin A detection.

Sensor type	Sample preparation	Electrolyte solution	Technique	Range (μM)	Sensitivity	LoD (μM)	Ref.
PPH/MWCNTs modified GCE	Dissolution of retinol in EtOH	Acetate buffer with 0.05% Triton X-100	SWV	5÷200	0.0573 μA/μM	0.8	[53]
β-cyclodextrin/ MWCNTs modified GCE	Dissolution of retinol in EtOH	0.1 M Britton–Robinson buffer solution with 0.02% SDS and 0.01% Triton X-100	SWV	6÷200	0.218 μA/μM	3.4	[54]
MWCNTs modified graphite electrode	Saponification of retinyl palmitate in alkaline EtOH solution	0.1 M $HClO_4$ in CH_3CN	CV	50÷1500	0.0057 μA/μM	40	[58]
SDS modified CPE	Dissolution of RETA in CH_3CN	0.1 M $LiClO_4$ in CH_3CN	DPV	1.5÷180	0.0161 μA/μM	0.46	[45]
PEDOT:PSS based OECT	Dissolution of RETA in the electrolyte solution	0.1 M $LiClO_4$ in EtOH/CH_3CN	PS	1÷1000	10 μA/decade	0.115	This work
PEDOT:PSS based OECT	Dissolution of RETA in the electrolyte solution	0.1 M $LiClO_4$ in EtOH/CH_3CN	PD	Linear: 50÷500 Logarithmic: 500÷1350	0.0459 μS/μM 40.7 μS/ decade	10	This work

LoD = limit of detection; PPH = poly(2,2′-(1,4-phenylenedivinylene)-bis-8-hydroxyquinaldine); MWCNTs = multi-walled carbon nanotubes; GCE = glassy carbon electrode; SDS = sodium dodecyl sulfate; CPE = carbon paste electrode; PEDOT:PSS = poly(3,4-ethylenedioxythiophene):poly(styrene sulfonate); OECT = organic electrochemical transistor; SWV = square wave voltammetry; CV = cyclic voltammetry; DPV = differential pulse voltammetry; PS = potentiostatic; PD = potentiodynamic.

nanomaterials modified electrodes and sophisticated voltammetric techniques [45,53,54]. In contrast, the detection carried out using a simple potentiostatic technique with our all-polymeric OECT sensor has shown to achieve the lowest LoD thanks to the amplification provided by the transistor structure. Despite the high performance, as thoroughly discussed, this approach is not selective. Instead, the OECT sensor used potentiodynamically is selective and offers one of the widest concentration ranges, but its LoD value is slightly lower than the one exhibited by a MWCNTs modified graphite electrode working in cyclic voltammetry [58]. Nevertheless, it is worth considering that this analytical method is the only one combining (i) simple analysis procedure (including sample preparation and analysis), with no need of sample pre-treatments or surfactants addition and application of complex waveforms during detection; (ii) simple sensor configuration based on the transistor architecture, which is compatible with large-scale production and miniaturisation by lithographic methods, as well as cheap and portable power supply and reading electronics, as it does not need a potentiostat.

3.6. Real samples analysis

In order to demonstrate the applicability of the OECT sensor to the analysis of real samples, the determination of Vitamin A in two commercial food additives was carried out, i.e., dry Vitamin A Acetate (RETA) 325 CWS/A and dry Vitamin A palmitate (REPA) 250 S/N. In the former, 11.18 wt% RETA is stabilized with Tocopherol and encapsulated in gum acacia, while in the latter 13.75 wt% REPA is stabilized with dibutylhydroxytoluene (BHT) and encapsulated in starch. The standard analytical technique for the analysis of food products is liquid chromatography, where a multi-step sample preparation is typically required to ensure complete extraction of the analyte, including direct solvent extraction or saponification [59], as well as enzymatic digestion [60], coupled to thermal/ultrasonic pretreatments. In contrast, a much simpler procedure was adopted for the electrochemical detection. First, two OECT sensors were calibrated for RETA and REPA, the latter compound showing a behavior similar to RETA at the OECT in the experimental conditions optimized for the selective detection of the acetate analog (Fig. S19). Then, the commercial powders were dispersed in distilled water to reach theoretical RETA and REPA concentrations of 10 mM and 8 mM, respectively. Controlled additions of the homogeneous milky-like dispersions were then performed directly into the electrochemical cell containing the organic solvent under stirring and the potentiodynamic detection was carried out, as described above. It is worth of note that each addition in the organic environment, corresponding to a theoretical concentration as shown in the legends of Fig. 6a and c, caused an immediate flocculation and all analyses were carried out in the presence of the solid residues floating inside the electrochemical cell. This phenomenon had no detrimental effect on the OECT sensor capability of detecting RETA and REPA (Fig. 6). In the case of 325 CWS/A (Fig. 6a and b), the presence of TCF as stabilizer was only detectable at the highest concentrations (Fig. S20), as evident from the g_m curves at around 0.8 V, however, without affecting the analytical signal thanks to the sensor selectivity. In the case of 250 S/N (Fig. 6c and d), no additional oxidation waves were detected in the potential window under investigation for REPA detection.

Table 2 reports the results obtained using the OECT sensor for the determination of RETA and REPA in the two commercial fortifiers. Very good match was found in both cases with the declared concentrations, demonstrating excellent sensing performances in the analysis of raw commercial products, without any pre-treatment or extraction procedure needed for the sample preparation.

The sensor behaviour was also assessed for the analysis of a commercial multivitamin powder containing more than 15 active compounds, including RETA, Vitamins D3, E, B1, B2, B3, B6, B9, B12, Vitamin C and mineral salts. In analogy with the fortifiers, the powder was simply solubilized in water and a controlled amount was added to the electrochemical cell. Despite the presence of suspended solid in the highly heterogeneous mixture obtained, the sensor response to the multivitamin premix clearly shows the presence of two peaks (Fig. 7, black curve). As confirmed by the analysis of the two individual premix components (Fig. S21), Vitamin E, which is present in the premix as Tocopheryl acetate, does not contribute to the sensor response, while the peak at 0.9 V was ascribed to the oxidation of Vitamin C. The latter gives rise to a broad peak at V_g values close to the oxidation potential of RETA and the molar concentration of Vitamin C is almost 100 times higher than RETA in the premix. However, despite (i) the heterogeneous sample solution, (ii) the presence of many other oxidizable fat and water soluble vitamins and (iii) the massive amount of Vitamin C, the sensor response to RETA additions remains linear, with very high recovery if compared to the calibration of the pure vitamin in the organic solvent (see for instance Fig. 6b), and does not show saturation, as evident especially after the subtraction of the matrix contribution (baseline subtraction, Fig. 7).

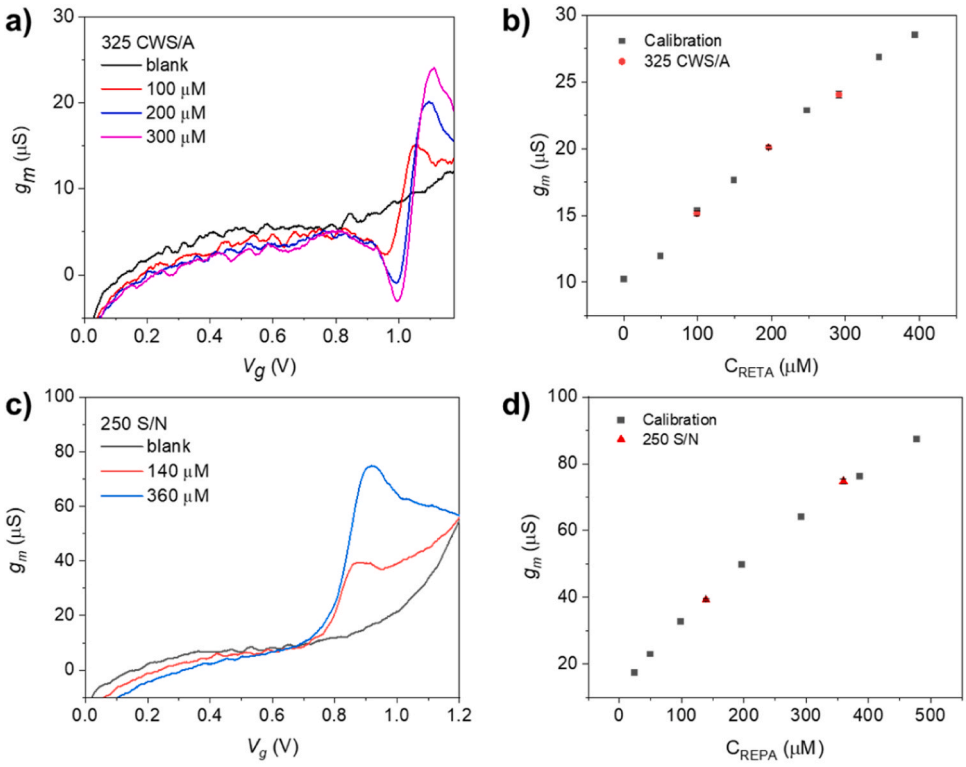

Fig. 6. Vitamin A detection in commercial food fortifiers. (a,b) Potentiodynamic analyses of the Retinyl acetate containing product (325 CWS/A) and (c,d) the Retinyl palmitate containing product (250 S/N) with a pre-calibrated OECT sensor (Au gate). Error bars represent the standard deviation calculated for N = 3 potentiodynamic cycles.

Table 2
Results of the analyses carried out on two commercial products.

Product	Vitamin A form	Declared concentration (%wt)	Calculated concentration (%wt ± SD)
325 CWS/A	RETA	11.18	11.0 ± 0.7
250 S/N	REPA	13.75	13.5 ± 0.5

4. Conclusion

Electrochemical sensors exhibit several advantages such as cost-effectiveness, ease of miniaturization, high sensitivity and versatility, which make them competitive among all electroanalytical tools not only for routinary analyses in the lab, but especially towards real-time, portable and Internet of Things applications. Several examples of electrochemical sensors have been reported so far for the detection of vitamins, including few transistor-based sensors, by which superior performances were achieved thanks to the amplification of the signal combined to the electrochemical transduction. However, fat-soluble vitamins detection with OECTs, and more in general the development of an OECT sensor working in organic media, were never explored so far by researchers. Due to the novelty of this topic, our investigation started from a thorough material and device characterization. To the best of our knowledge, the OECT behavior was assessed in organic environment for the first time, replacing the watery electrolyte solutions that are familiar to bioelectronic applications. Moreover, the capability of the transistor to work as an electrochemical sensor in organic medium was demonstrated through the successful quantification of retinyl acetate, exploiting both potentiostatic and potentiodynamic approaches. Upon optimization of the OECT structure and potentiodynamic parameters, we were able to resolve the signals ascribed to Vitamin A and E in a binary mixture. Furthermore, excellent performances were found when analyzing commercial food fortifiers and a multivitamin premix powder,

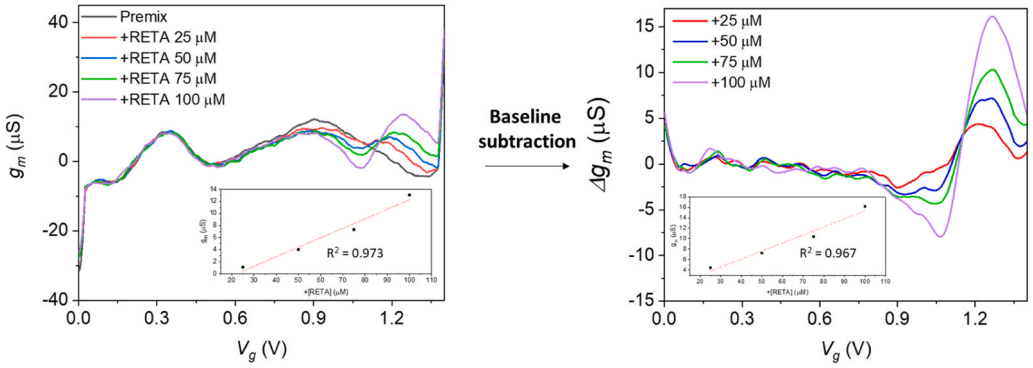

Fig. 7. Sensor response in a commercial multivitamin premix upon controlled RETA additions, before and after baseline subtraction (insets: calibration curves).

without any pre-treatment or extraction procedure employed for the sample preparation. In our opinion, this work reports encouraging results to bring these bioelectronic devices beyond the watery part of life and biology, where they have already proved to provide uniquely performing electrochemical interfaces. Nevertheless, this work represents a step forward in the real-time sensing of vitamins, where portable and smartphone-interfaced devices have not been assessed yet. To this regard, the OECT is a robust and low power consuming platform that not only is compatible with portable setups, but also works reliably in complex and untreated matrices and might also be optimized for the simultaneous detection of both water-soluble and fat-soluble vitamins.

CRediT authorship contribution statement

Luca Salvigni: Investigation, Formal analysis, Validation, Data curation, Writing – original draft. **Federica Mariani:** Methodology, Investigation, Supervision, Conceptualization, Writing – review & editing. **Isacco Gualandi:** Methodology, Supervision. **Francesco Decataldo:** Investigation – OECTs fabrication. **Marta Tessarolo:** Formal analysis. **Domenica Tonelli:** Supervision, Funding acquisition. **Beatrice Fraboni:** Supervision, Funding acquisition. **Erika Scavetta:** Supervision, Funding acquisition.

Declaration of Competing Interest

The authors declare that they have no known competing financial interests or personal relationships that could have appeared to influence the work reported in this paper.

Data Availability

Data will be made available on request.

Acknowledgements

The authors are grateful to DSM Nutritional Products for the technical and economic support received in the framework of the research project entitled "Development of a transistor-based sensor for the detection of liposoluble vitamins in organic solvents".

Appendix A. Supporting information

Supplementary data associated with this article can be found in the online version at doi:10.1016/j.snb.2023.134313.

References

[1] R. Porada, B. Baś, Separation of the overlapped vitamin B1 and B3 voltammetric peaks by means of continuous wavelet transform and differentiation, Mon. Für Chem. - Chem. Mon. 152 (2021) 1107–1117, https://doi.org/10.1007/s00706-021-02788-6.
[2] B. Brunetti, Recent advances in electroanalysis of vitamins, Electroanalysis 28 (2016) 1930–1942, https://doi.org/10.1002/elan.201600097.
[3] A.J. Didier, J. Stiene, L. Fang, D. Watkins, L.D. Dworkin, J.F. Creeden, Antioxidant and anti-tumor effects of dietary vitamins A, C, and E, Antioxidants 12 (2023) 632, https://doi.org/10.3390/antiox12030632.
[4] L. Huang, S. Tian, W. Zhao, K. Liu, J. Guo, Electrochemical vitamin sensors: a critical review, Talanta 222 (2021), 121645, https://doi.org/10.1016/j.talanta.2020.121645.
[5] C.J. Blake, Analytical procedures for water-soluble vitamins in foods and dietary supplements: a review, Anal. Bioanal. Chem. 389 (2007) 63–76, https://doi.org/10.1007/s00216-007-1309-9.
[6] T.C. Canevari, F.H. Cincotto, R. Landers, S.A.S. Machado, Synthesis and characterization of α-nickel (II) hydroxide particles on organic-inorganic matrix and its application in a sensitive electrochemical sensor for vitamin D determination, Electro Acta 147 (2014) 688–695, https://doi.org/10.1016/j.electacta.2014.10.012.
[7] H. Bora, D. Mandal, A. Chandra, High-performance, nitrogen-doped, carbon-nanotube-based electrochemical sensor for vitamin D3 detection, ACS Appl. Bio Mater. 5 (2022) 1721–1730, https://doi.org/10.1021/acsabm.2c00094.
[8] A. Lermo, S. Fabiano, S. Hernández, R. Galve, M.-P. Marco, S. Alegret, M. I. Pividori, Immunoassay for folic acid detection in vitamin-fortified milk based on electrochemical magneto sensors, Biosens. Bioelectron. 24 (2009) 2057–2063, https://doi.org/10.1016/j.bios.2008.10.020.
[9] S.A. Shahamirifard, M. Ghaedi, A new electrochemical sensor for simultaneous determination of arbutin and vitamin C based on hydroxyapatite-ZnO-Pd nanoparticles modified carbon paste electrode, Biosens. Bioelectron. 141 (2019), 111474, https://doi.org/10.1016/j.bios.2019.111474.
[10] J. Ma, L. Shen, Y. Jiang, H. Ma, F. Lv, J. Liu, Y. Su, N. Zhu, Wearable self-powered smart sensors for portable nutrition monitoring, Anal. Chem. 94 (2022) 2333–2340, https://doi.org/10.1021/acs.analchem.1c05189.
[11] S. Wadhwa, A.T. John, S. Nagabooshanam, A. Mathur, J. Narang, Graphene quantum dot-gold hybrid nanoparticles integrated aptasensor for ultra-sensitive detection of vitamin D3 towards point-of-care application, Appl. Surf. Sci. 521 (2020), 146427, https://doi.org/10.1016/j.apsusc.2020.146427.
[12] J.R. Sempionatto, L.C. Brazaca, L. García-Carmona, G. Bolat, A.S. Campbell, A. Martin, G. Tang, R. Shah, R.K. Mishra, J. Kim, V. Zucolotto, A. Escarpa, J. Wang, Eyeglasses-based tear biosensing system: Non-invasive detection of alcohol, vitamins and glucose, Biosens. Bioelectron. 137 (2019) 161–170, https://doi.org/10.1016/j.bios.2019.04.058.
[13] A. Lesch, F. Cortés-Salazar, V. Amstutz, P. Tacchini, H.H. Girault, Inkjet printed nanohydrogel coated carbon nanotubes electrodes for matrix independent sensing, Anal. Chem. 87 (2015) 1026–1033, https://doi.org/10.1021/ac503748g.
[14] Y. Yang, J. Zhou, H. Zhang, P. Gai, X. Zhang, J. Chen, Electrochemical evaluation of total antioxidant capacities in fruit juice based on the guanine/graphene nanoribbon/glassy carbon electrode, Talanta 106 (2013) 206–211, https://doi.org/10.1016/j.talanta.2012.12.030.
[15] E. Kuraya, S. Nagatomo, K. Sakata, D. Kato, O. Niwa, T. Nishimi, M. Kunitake, Simultaneous electrochemical analysis of hydrophilic and lipophilic antioxidants in bicontinuous microemulsion, Anal. Chem. 87 (2015) 1489–1493, https://doi.org/10.1021/ac5044576.
[16] L. Zhang, G. Wang, D. Wu, C. Xiong, L. Zheng, Y. Ding, H. Lu, G. Zhang, L. Qiu, Highly selective and sensitive sensor based on an organic electrochemical transistor for the detection of ascorbic acid, Biosens. Bioelectron. 100 (2018) 235–241, https://doi.org/10.1016/j.bios.2017.09.006.
[17] F. Decataldo, F. Bonafè, F. Mariani, M. Serafini, M. Tessarolo, I. Gualandi, E. Scavetta, B. Fraboni, Oxygen gas sensing using a hydrogel-based organic electrochemical transistor for work safety applications, Polymers 14 (2022) 1022, https://doi.org/10.3390/polym14051022.
[18] C. Liao, M. Zhang, L. Niu, Z. Zheng, F. Yan, Organic electrochemical transistors with graphene-modified gate electrodes for highly sensitive and selective dopamine sensors, J. Mater. Chem. B 2 (2014) 191–200, https://doi.org/10.1039/C3TB21079K.
[19] F. Mariani, T. Quast, C. Andronescu, I. Gualandi, B. Fraboni, D. Tonelli, E. Scavetta, W. Schuhmann, Needle-type organic electrochemical transistor for spatially resolved detection of dopamine, Microchim. Acta 187 (2020) 378, https://doi.org/10.1007/s00604-020-04352-1.
[20] F. Mariani, I. Gualandi, W. Schuhmann, E. Scavetta, Micro- and nano-devices for electrochemical sensing, Microchim. Acta 189 (2022) 459, https://doi.org/10.1007/s00604-022-05548-3.
[21] S.T. Keene, C. Lubrano, S. Kazemzadeh, A. Melianas, Y. Tuchman, G. Polino, P. Scognamiglio, L. Cinà, A. Salleo, Y. van de Burgt, F. Santoro, A biohybrid synapse with neurotransmitter-mediated plasticity, Nat. Mater. 19 (2020) 969–973, https://doi.org/10.1038/s41563-020-0703-y.
[22] Y. van de Burgt, E. Lubberman, E.J. Fuller, S.T. Keene, G.C. Faria, S. Agarwal, M. J. Marinella, A. Alec Talin, A. Salleo, A non-volatile organic electrochemical device as a low-voltage artificial synapse for neuromorphic computing, Nat. Mater. 16 (2017) 414–418, https://doi.org/10.1038/nmat4856.
[23] M. Ramuz, A. Hama, J. Rivnay, P. Leleux, R.M. Owens, Monitoring of cell layer coverage and differentiation with the organic electrochemical transistor, J. Mater. Chem. B 3 (2015) 5971–5977, https://doi.org/10.1039/C5TB00922G.
[24] P. Lin, F. Yan, J. Yu, H.L.W. Chan, M. Yang, The application of organic electrochemical transistors in cell-based biosensors, Adv. Mater. 22 (2010) 3655–3660, https://doi.org/10.1002/adma.201000971.
[25] V.F. Curto, M.P. Ferro, F. Mariani, E. Scavetta, R.M. Owens, A planar impedance sensor for 3D spheroids, Lab Chip 18 (2018) 933–943, https://doi.org/10.1039/C8LC00067K.
[26] F. Bonafè, F. Decataldo, I. Zironi, D. Remondini, T. Cramer, B. Fraboni, AC amplification gain in organic electrochemical transistors for impedance-based single cell sensors, Nat. Commun. 13 (2022) 5423, https://doi.org/10.1038/s41467-022-33094-2.
[27] A.B. Woeppel, J. Schaefer, H.J. Kim, B.W. Boudouris, S.P. Beaudoin, Ion-selective organic electrochemical transistor sensors using molecularly imprinted polymers, ACS Appl. Polym. Mater. 4 (2022) 6667–6674, https://doi.org/10.1021/acsapm.2c01030.
[28] I. Gualandi, M. Tessarolo, F. Mariani, D. Arcangeli, L. Possanzini, D. Tonelli, B. Fraboni, E. Scavetta, Layered double hydroxide-modified organic electrochemical transistor for glucose and lactate biosensing, Sensors 20 (2020) 3453, https://doi.org/10.3390/s20123453.
[29] F. Mariani, I. Gualandi, M. Tessarolo, B. Fraboni, E. Scavetta, C. Industriale, T. Montanari, U. Bologna, V. Risorgimento, PEDOT: dye-based, flexible organic electrochemical transistor for highly sensitive pH monitoring, Appl. Mater. Interfaces 10 (2018) 22474–22484, https://doi.org/10.1021/acsami.8b04970.
[30] I. Gualandi, E. Scavetta, F. Mariani, D. Tonelli, M. Tessarolo, B. Fraboni, All poly (3,4-ethylenedioxythiophene) organic electrochemical transistor to amplify amperometric signals, Electro Acta 268 (2018) 476–483, https://doi.org/10.1016/j.electacta.2018.02.091.

[31] I. Gualandi, M. Tessarolo, F. Mariani, D. Tonelli, B. Fraboni, E. Scavetta, Organic electrochemical transistors as versatile analytical potentiometric sensors, Front Bioeng. Biotechnol. 7 (2019) 354, https://doi.org/10.3389/fbioe.2019.00354.
[32] X. Qing, Y. Wang, Y. Zhang, X. Ding, W. Zhong, D. Wang, W. Wang, Q. Liu, K. Liu, M. Li, Z. Lu, Wearable fiber-based organic electrochemical transistors as a platform for highly sensitive dopamine monitoring, ACS Appl. Mater. Interfaces 11 (2019) 13105–13113, https://doi.org/10.1021/acsami.9b00115.
[33] S. Demuru, J. Kim, M. el Chazli, S. Bruce, M. Dupertuis, P.-A. Binz, M. Saubade, C. Lafaye, D. Briand, Antibody-coated wearable organic electrochemical transistors for cortisol detection in human sweat, ACS Sens 7 (2022) 2721–2731, https://doi.org/10.1021/acssensors.2c01250.
[34] I. Gualandi, M. Marzocchi, E. Scavetta, M. Calienni, A. Bonfiglio, B. Fraboni, A simple all-PEDOT:PSS electrochemical transistor for ascorbic acid sensing, J. Mater. Chem. B 3 (2015) 6753–6762, https://doi.org/10.1039/C5TB00916B.
[35] I. Gualandi, D. Tonelli, F. Mariani, E. Scavetta, M. Marzocchi, B. Fraboni, Selective detection of dopamine with an all PEDOT:PSS Organic Electrochemical Transistor, Sci. Rep. 6 (2016) 35419, https://doi.org/10.1038/srep35419.
[36] L. Contat-Rodrigo, C. Pérez-Fuster, J.V. Lidón-Roger, A. Bonfiglio, E. García-Breijo, Screen-printed organic electrochemical transistors for the detection of ascorbic acid in food, Org. Electron 45 (2017) 89–96, https://doi.org/10.1016/j.orgel.2017.02.037.
[37] L. Zhang, G. Wang, D. Wu, C. Xiong, L. Zheng, Y. Ding, H. Lu, G. Zhang, L. Qiu, Highly selective and sensitive sensor based on an organic electrochemical transistor for the detection of ascorbic acid, Biosens. Bioelectron. 100 (2018) 235–241, https://doi.org/10.1016/j.bios.2017.09.006.
[38] M. Sophocleous, L. Contat-Rodrigo, E. García-Breijo, J. Georgiou, Organic electrochemical transistors as an emerging platform for bio-sensing applications: a review, IEEE Sens J. 21 (2021) 3977–4006, https://doi.org/10.1109/JSEN.2020.3033283.
[39] L. Bai, C.G. Elósegui, W. Li, P. Yu, J. Fei, L. Mao, Biological applications of organic electrochemical transistors: electrochemical biosensors and electrophysiology recording, Front Chem 7 (2019), https://doi.org/10.3389/fchem.2019.00313.
[40] J. Rivnay, S. Inal, A. Salleo, R.M. Owens, M. Berggren, G.G. Malliaras, Organic electrochemical transistors, Nat. Rev. Mater. 3 (2018) 17086, https://doi.org/10.1038/natrevmats.2017.86.
[41] A.D. McNaught, A. Wilkinson. The IUPAC Compendium of Chemical Terminology, second ed., Blackwell Scientific Publications,, Oxford, 1997 https://doi.org/10.1351/goldbook.
[42] E. van Wayenbergh, J. Verheijen, N.A. Langenaeken, I. Foubert, C.M. Courtin, A simple method for analysis of vitamin A palmitate in fortified cereal products using direct solvent extraction followed by reversed-phase HPLC with UV detection, Food Chem. 404 (2023), 134584, https://doi.org/10.1016/j.foodchem.2022.134584.
[43] Y.S. Tan, D. Urbančok, R.D. Webster, Contrasting voltammetric behavior of different forms of vitamin A in aprotic organic solvents, J. Phys. Chem. B 118 (2014) 8591–8600, https://doi.org/10.1021/jp505456q.
[44] R.D. Webster, Voltammetry of the liposoluble vitamins (A, D, E and K) in organic solvents, Chem. Rec. 12 (2012) 188–200, https://doi.org/10.1002/tcr.201100005.
[45] S. Žabčíková, T. Mikysek, L. Červenka, M. Sýs, Electrochemical study and determination of all-trans retinol at carbon paste electrode modified by surfactant, Food Technol. Biotechnol. 56 (2018) 337–343, https://doi.org/10.17113/ftb.56.03.18.5618.
[46] A. Masek, E. Chrzescijanska, M. Zaborski, Voltammetric and FTIR spectroscopic studies of the oxidation of retinyl propionate at Pt electrode in non-aqueous media, Int J. Electrochem Sci. 9 (2014) 6809–6820.
[47] D.A.J. Rand, R. Woods, Determination of the surface composition of smooth noble metal alloys by cyclic voltammetry, J. Electro Chem. Interfacial Electrochem 36 (1972) 57–69, https://doi.org/10.1016/S0022-0728(72)80445-5.
[48] I. Gualandi, M. Marzocchi, A. Achilli, D. Cavedale, A. Bonfiglio, B. Fraboni, Textile organic electrochemical transistors as a platform for wearable biosensors, Sci. Rep. 6 (2016) 33637, https://doi.org/10.1038/srep33637.
[49] F. Mariani, F. Conzuelo, T. Cramer, I. Gualandi, L. Possanzini, M. Tessarolo, B. Fraboni, W. Schuhmann, E. Scavetta, Microscopic determination of carrier density and mobility in working organic electrochemical transistors, Small 15 (2019) 1902534, https://doi.org/10.1002/smll.201902534.
[50] N. EFSA, Panel on dietetic products and allergies (NDA), scientific opinion on dietary reference values for vitamin A, EFSA J. 13 (2015) 4028, https://doi.org/10.2903/j.efsa.2015.4028.
[51] A.S. Hombali, J.A. Solon, B.T. Venkatesh, N.S. Nair, J.P. Peña-Rosas, Fortification of staple foods with vitamin A for vitamin A deficiency, Cochrane Database Syst. Rev. 5 (2019) CD010068, https://doi.org/10.1002/14651858.CD010068.pub2.
[52] C.M. Proctor, J. Rivnay, G.G. Malliaras, Understanding volumetric capacitance in conducting polymers, J. Polym. Sci. B Polym. Phys. 54 (2016) 1433–1436, https://doi.org/10.1002/polb.24038.
[53] H. Filik, A.A. Avan, S. Aydar, Simultaneous electrochemical determination of α -tocopherol and retinol in micellar media by a Poly(2,2′-(1,4 Phenylenedivinylene)-bis-8-Hydroxyquinaldine)-Multiwalled Carbon Nanotube Modified Electrode, Anal. Lett. 49 (2016) 1240–1257, https://doi.org/10.1080/00032719.2015.1094665.
[54] A.A. Avan, H. Filik, Simultaneous determination of fat-soluble vitamins by using modified glassy carbon electrode, Russ. J. Electrochem. 57 (2021) 858–871, https://doi.org/10.1134/S1023193521080048.
[55] J. Thangphatthanarungruang, A. Ngamaroonchote, R. Laocharoensuk, C. Chotsuwan, W. Siangproh, A novel electrochemical sensor for the simultaneous determination of fat-soluble vitamins using a screen-printed graphene/nafion electrode, Key Eng. Mater. 777 (2018) 597–601, https://doi.org/10.4028/www.scientific.net/KEM.777.597.
[56] D.A. Bernards, D.J. Macaya, M. Nikolou, J.A. DeFranco, S. Takamatsu, G. G. Malliaras, Enzymatic sensing with organic electrochemical transistors, J. Mater. Chem. 18 (2008) 116–120, https://doi.org/10.1039/B713122D.
[57] W. Wei Yao, H. Mei Peng, R.D. Webster, Electrochemistry of α-tocopherol (Vitamin E) and α-tocopherol quinone films deposited on electrode surfaces in the presence and absence of lipid multilayers, J. Phys. Chem. C. 113 (2009) 21805–21814, https://doi.org/10.1021/jp9079124.
[58] G. Ziyatdinova, M. Morozov, H. Budnikov, MWNT-modified electrodes for voltammetric determination of lipophilic vitamins, J. Solid State Electrochem. 16 (2012) 2441–2447, https://doi.org/10.1007/s10008-011-1581-7.
[59] L. Ye, W.O. Landen, R.R. Eitenmiller, Liquid chromatographic analysis of all-trans-retinyl palmitate, β-Carotene, and Vitamin E in fortified foods and the extraction of encapsulated and nonencapsulated retinyl palmitate, J. Agric. Food Chem. 48 (2000) 4003–4008, https://doi.org/10.1021/jf000341w.
[60] G.M. Ware, G.W. Chase, R.R. Eitenmiller, A.R. Long, Determination of vitamin K1 in medical foods by liquid chromatography with postcolumn reduction and fluorometric detection, J. AOAC Int 83 (2000) 957–962, https://doi.org/10.1093/jaoac/83.4.957.

Luca Salvigni obtained his Master's degree in Industrial Chemistry summa cum laude in 2020 from the University of Bologna, with a thesis on electrochemistry. He worked for one year as a research fellow on a project funded by DSM Nutritional Products for the development of an Organic Electrochemical Transistor (OECT) based sensor. He is currently a PhD student at King Abdullah University of Science and Technology (KAUST), where he is working on the study of fundamental working mechanisms of OECT for sensing and materials characterization.

Federica Mariani obtained her Master's degree in Industrial Chemistry summa cum laude (2016) and her PhD in Chemical Sciences (2020) from the University of Bologna, after research stays in France (Centre Microélectronique de Provence, Gardanne) and Germany (Center for Electrochemical Sciences, Ruhr-Universität Bochum, Bochum). She is currently a junior reasearcher in Analytical Chemistry at the University of Bologna and her research interest addresses the development of bioelectronic interfaces, including transistor-based sensors and wearable devices.

Isacco Gualandi graduated in Industrial Chemistry summa cum laude in 2009 and he accomplished his PhD studies in Chemical Sciences in 2013 at the University of Bologna. After a period of post-doctoral fellowships at the Departments of Physics and Industrial Chemistry, he worked as a researcher. Now he is an associate professor in analytical chemistry (university of Bologna) and his research activity focuses on the development of innovative electrochemical sensors based on both inorganic and organic materials.

Francesco Decataldo obtained his master's degree in physics summa cum laude (2016) and his PhD in Physics (2020) from the Department of Physics and Astronomy of the University of Bologna (Italy), after research stays at the Department of Chemical Engineering and Biotechnology in Cambridge (United Kingdom). He is currently employed as a Junior Assistant Professor at the Department of Medical and Surgical Sciences, working on advanced microscopy for biological analysis, micropatterning on different substrates and electrical/morphological characterizations of organic polymers. His research interests involve electrochemical biosensors, devices for tissue engineering, wearable sensors.

Marta Tessarolo received the PhD (2016) in the Department of Physics and Astronomy at University of Bologna. Currently she works as laboratory technician in the Department of Physics. Her research interests include organic semiconductors, wearable textile sensors, electrochemical transistors and bioelectronics.

Domenica Tonelli graduated in Chemistry *summa cum laude* at the Institute of Chemistry "G. Ciamician" of Bologna University. In 1982 she joined the Faculty of Farmacy as researcher. In 1992 she joined the Faculty of Industrial Chemistry as associated professor, and later as Full professor in Analytical Chemistry. Member of the Italian Chemical Society and The International Society of Electrochemistry, she continues her scientific work as Alma Mater professor after her retirement. She is co-author of more than 250 papers published in international journals. Her present research activity focuses on the development of innovative electrochemical sensors based on both inorganic and organic materials and on the synthesis and characterization of materials for catalytic and energy storage applications.

Beatrice Fraboni is a Full Professor of Physics at the University of Bologna. She is the Director of the "Collegio Superiore Irnerio" (www.collegio.unibo.it/en) and is the Head of the "Semiconductor Physics Group" (https://site.unibo.it/semiconductor-physics/en) of the Department of Physics and Astronomy. Her research activity focuses on the analysis and characterization of the electrical transport properties of organic and inorganic semiconducting materials and of advanced (bio)electronic devices.

Erika Scavetta holds a PhD in Chemical Sciences and she is a Full Professor of Analytical Chemistry at the University of Bologna. She is Director of First Cycle Degree in Chemistry and Technologies for the Environment and Materials and is the Head of the 'Analytical Chemistry Group' of the Department of Industrial Chemistry 'Toso Montanari'. Her research activity focuses on the development of innovative electrochemical sensors based on both inorganic and organic materials.